Electric Field–induced Redistribution and Postfield Relaxation of Low Density Lipoprotein Receptors on Cultured Human Fibroblasts

DAVID W. TANK, W. J. FREDERICKS, L. S. BARAK, and W. W. WEBB

Department of Physics and School of Applied and Engineering Physics, Cornell University, Ithaca, New York 14853. D. W. Tank's present address is Department of Molecular Biophysics, AT&T Bell Laboratories, Murray Hill, New Jersey 07974. W. J. Fredericks' present address is Department of Pharmacology, Roswell Park Memorial Institute, Buffalo, New York 14263. L. S. Barak's present address is Department of Pediatrics, University of South Florida, Tampa, Florida 33606.

ABSTRACT The lateral mobility of unliganded low density lipoprotein–receptor (LDL-R) on the surface of human fibroblasts has been investigated by studying the generation and relaxation of concentration differences induced by exposure of the cultured cells to steady electric fields. The topographic distribution of receptors was determined by fluorescence microscopy of cells labeled with the intensely fluorescent, biologically active LDL derivative dioctadecylindolcarbocyanine LDL (dil(3)-LDL), or with native LDL and anti-LDL indirect immunofluorescence. Exposure of the LDL-receptor-internalization defective J. D. cells (GM2408A) to an electric field of 10 V/cm for 1 h at 22°C causes >80% of the cells to have an asymmetric distribution of LDL-R; receptors accumulate at the more negative pole of the cell. In contrast, only 20% of LDL-internalization normal GM3348 cells exposed to identical conditions have asymmetrical distributions. Phase micrographs taken during electric-field exposure rule out cell movement as the responsible mechanism for the effect. In both cell types, postfield labeling with the F-actin-specific fluorescent probe nitrobenzoxadiazole-phallacidin shows that no topographic alteration of the actin cytoskeleton accompanies the redistribution of cell surface LDL-Rs, and indirect immunofluorescence labeling of the coat protein clathrin shows that coated pits do not redistribute asymmetrically. Measurements of the postfield relaxation in the percentage of GM2408A cells showing an asymmetric distribution allow an estimate of the effective postfield diffusion coefficient of the unliganded LDL-R. At 37°C, $D = 2.0 \times 10^{-9}$ cm^2/s, decreasing to 1.1×10^{-9} cm^2/s at 22°C, and $D = 3.5 \times 10^{-10}$ cm^2/s at 10°C. These values are substantially larger than those measured by photobleaching methods for the LDL-R complexed with dil(3)-LDL on intact cells, but are comparable to those measured on membrane blebs, and are consistent with diffusion coefficients measured for other unliganded integral membrane receptor proteins by postfield-relaxation methods.

The low density lipoprotein particle binds with high affinity to the cell surface low density lipoprotein–receptor (LDL-R),[1] and the resulting complex is internalized at coated regions of the plasma membrane (1–3). Internalization at coated pits also follows the cell surface receptor-mediated binding of

[1] *Abbreviations used in this paper:* %A, percentage of cells showing an asymmetric distribution; buffer A, a solution of 10 mM HEPES, pH 7.3; buffer B, a solution of 0.15 M NaCl, 2 mM $MgCl_2$, 10 mM NaP_i, pH 7.3; dil(3)-LDL, intensely fluorescent, biologically active LDL derivative dioctadecylindolcarbocyanine LDL; FCS, fetal calf serum; GM2408A, an LDL-R internalization-deficient human fibroblast cell line, also known as J. D. cells; GM3348, a normal cell line of human fibroblasts; LDL-R, low density lipoprotein–receptor; LDL-RC, LDL receptor complex; NBD, nitrobenzoxadiazole; PBS+, phosphate-buffered saline containing Ca^{2+} and Mg^{2+}.

THE JOURNAL OF CELL BIOLOGY · VOLUME 101 JULY 1985 148–157

other important plasma proteins such as insulin and epidermal growth factor (4, 5). However, for a normal cell line of human fibroblasts (GM3348), the LDL-R is believed to be located in the coated regions before LDL binding (6, 7), undergoing continuous internalization and recycling, whereas in the case of insulin and EGF, binding to randomly dispersed receptors is followed by clustering at the coated region and subsequent internalization (8, 9).

J. D. cells (GM2408A), a mutant human fibroblast cell line that does not internalize LDL by the normal sequence, have been characterized by Brown and Goldstein (10, 11). The LDL-R complexes are dispersed nearly randomly on GM2408A cells. In contrast, on GM3348 cells, they are concentrated at coated pits. Genetic and biochemical studies have suggested that the GM2408A lesion is caused by a single-point mutation that destroys the ability of the LDL-R to associate with a coated region of the membrane even though its affinity for LDL is unimpaired (7).

The internalization lesion in GM2408A cells could also have been the result of the lateral immobilization of the LDR-R in the plasma membrane. However, using the technique of pattern fluorescence photobleaching recovery, recent measurements in our laboratory of the lateral mobility of the LDL-R-complex (LDL-RC) formed by binding dioctadecylindolcarbocyanine LDL (dil(3)-LDL) to the LDL-R have shown diffusion on the GM2408A cell surface with $D = 2.5 \times 10^{-11}$ cm^2/s at 22°C (12, 13). This diffusion coefficient is sufficient so that during the 5-min average lifetime of a coated pit, diffusive processes are fast enough for the complex to locate a coated region. Thus, the hypothesis that receptor immobilization causes the internalization deficiency of these cells is not tenable.

Although this value of D for the LDL-RC on the GM2408A cell surface is sufficiently large so that receptor-coated pit interactions are not diffusion restricted, it also suggests that there is nevertheless a constraint on LDL-RC lateral mobility. Diffusion of large integral membrane proteins reconstituted into phospholipid model membranes show $D \sim 10^{-8}$ cm^2/s, about what is observed for lipid analogues in the same systems (see, for example references 14 and 15). Also, our recent measurements of enhanced diffusibility of identified receptors on the cell surface membrane that has been physically decoupled from the cytoplasm by the formation of blebs (16, 17) demonstrate that large integral membrane proteins can diffuse in situ, provided they are unrestrained, at rates ($D \sim 2$–5×10^{-9} cm^2/s) only slightly slower than reconstituted proteins in pure lipid model systems. In particular, analysis of video recordings of Brownian motion of the LDL-RC on GM2408A blebs indicates much faster diffusion than on the normal cell surface, with $D = 2.5 \times 10^{-9}$ cm^2/s (13). These diffusion experiments involving the LDL-R have measured the diffusibility of LDL-RC, the liganded form of the LDL-R, with the large, highly fluorescent, LDL particle complexed with the receptor. Due to the low surface density of the LDL-R and the lack of a direct, low molecular weight label of sufficient fluorescence intensity, we have turned to alternative techniques to study the cell surface mobility of the unliganded receptor.

The photobleaching technique creates an asymmetric distribution of diffusive species by a patterned destruction of chromophore, and the rate of recovery to a constant distribution under the induced concentration gradients provides a measure of the lateral diffusion coefficient (18, 19). An asymmetric distribution of diffusive species can also be induced by exposure of cells to a constant electric field. This redistribution of membrane components occurs by a process involving electrophoresis (20, 21) and/or electro-osmosis (22). Like photobleaching, the rate of the relaxation of the resulting concentration gradients of cell surface components provides a measure of the lateral diffusion coefficient (23). One important difference between photobleaching and electric field–induced redistribution experiments is that for the latter, diffusion can be occurring for the unlabeled species. Concentration distributions can be determined at specific time points by fixation and subsequent labeling.

In this paper, we present the results of electric field redistribution experiments on GM2408A and GM3348 fibroblasts that probe the association of the LDL-R with coated membranes and estimate the postfield lateral mobility of the LDL-R in the absence of LDL.

MATERIALS AND METHODS

Cells and Growth Conditions: GM3348 and GM2408A cell lines, and GM2000, an LDL-binding-defective human fibroblastic cell line, were obtained from the Human Genetic Mutant Cell Repository (Camden, NJ). Cells were grown in Ham's F-12 growth medium (Flow Laboratories, Inc., McLean, VA) supplemented with 10% fetal calf serum (FCS; Gibco Laboratories, Grand Island, NY), as described previously (24). For experiments, cells were plated onto 22 × 30-mm No. 1 glass coverslips, and upregulation of the number of LDL receptors per cell (25) was accomplished by removing the growth medium after 24–48 h, washing the cells once with Medium 199 (Gibco Laboratories), and adding Ham's F-12 growth medium supplemented with 10% delipidated FCS, prepared as described (26). Cells were incubated in this delipidated growth medium 40–70 h before being used for experiments.

Dil(3)-LDL: Preparation and Cell Labeling: LDL purification, reconstitution with dil(3), and tests of binding specificity were performed as described previously (24). For live cell labeling with dil(3)-LDL, all prefixation steps were done with cells and solutions maintained at 4°C. Cells were first washed twice in Medium 199 supplemented with 10 mM HEPES at pH 7.3 (buffer A), followed by incubation for 15 min with buffer A containing 12 μg/ml dil(3)-LDL. After three washes with phosphate-buffered saline containing Ca^{2+} and Mg^{2+} (PBS+; Gibco Laboratories), nonspecific labeling was removed by incubation for 10 min in Hanks' balanced salt solution (Gibco Laboratories) supplemented with 2 mg/ml bovine serum albumin (BSA; Sigma Chemical Co., St. Louis, MO), 2 mM $CaCl_2$, and 10 mM Tris at pH 7.3. A wash in buffer A was followed by fixation at 23°C in a 3–4% solution of formaldehyde in PBS+ for 5–15 min. Fixation was followed by three washes in PBS+ or buffer A. With the edges being supported by thin wax paper strips, the coverslip was then placed cell-side-down over the surface of a glass slide. The included volume was filled with PBS+ or buffer A, and the edges were sealed with molten wax.

Double Labeling of F-Actin and LDL-R: All prefixation cell handling was performed at 4°C. Cells were washed twice in buffer A and soaked for 15 min in a solution of 10% FCS-LDL in Medium 199, pH 7.3. (For coverslips that had been exposed to the standard electrophoresis conditions [see below], this soak helped to prevent nonspecific binding of LDL to the glass, which was higher than what was observed on control coverslips not exposed to the electric field.) Cells were then washed three times in buffer A and incubated for 15 min with 12 μg/ml unlabeled LDL in buffer A. Next, the cells were incubated with affinity purified rabbit anti-human beta lipoprotein antibody (Cappel Laboratories, Cochranville, PA) at a 1:500 dilution in buffer A for 40 min. This was followed by three washes in buffer A and incubation with affinity purified biotinylated goat anti-rabbit IgG antibody (Vector Laboratories, Inc., Burlingame, CA) at 38 μg/ml in buffer A for 40 min. After three washes in buffer A, fluorescence labeling was accomplished by incubation with rhodamine-labeled avidin D (Vector Laboratories, Inc.) at 10 μg/ml in buffer A for 40 min. After a triple wash in buffer A, cells were soaked in Hanks' balanced salt solution containing 2 mg/ml BSA, 2 mM $CaCl_2$, and 10 mM Tris pH 7.3. Cells were then fixed in 3.7% formaldehyde for 15 min at 23°C and washed three times in PBS+. After this initial fixation of the LDL-R labeling, cells were simultaneously refixed, extracted, and labeled with nitrobenzoxadiazole (NBD)-phallacidin as follows. A solution of 4% formaldehyde containing 10 μg/ml of L-alpha-lysophosphatidylcholine palmitoyl (Sigma Chemical Co.) and 125 ng/ml of NBD-phallacidin (prepared as in reference 27) was applied to the cells for 50 min at 4°C. After a triple wash in PBS+, there was a 1-h incubation with

a solution of NBD-phallacidin at 125 ng/ml in PBS+. The coverslips were given a final wash in PBS+ and mounted for viewing as described in the second section of Materials and Methods.

Antibody Labeling of Clathrin: Rabbit anti-clathrin antibody was the generous gift Drs. Michael Brown, Joseph Goldstein, and Richard Anderson (University of Texas Health Science Center at Dallas, Dallas, Texas). For clathrin labeling, cells were washed twice in 0.15 M NaCl, 2 mM $MgCl_2$ and 10 mM NaP_i, pH 7.3 (buffer B) and then fixed at 23°C for 10 min in buffer B containing 3% formaldehyde. After a wash in buffer B, cells were incubated with a solution of 0.05% Triton X-100 in buffer B at −10°C for 5 min. After washing in buffer B, cells were incubated with rabbit anti-clathrin antibody at 0.4 mg/ml for 1 h at 37°C. This was followed by four 15-min soaks in buffer B. To visualize the rabbit anti-clathrin distribution, two strategies were employed. Either the cells were incubated with rhodamine-labeled goat anti-rabbit IgG (Cappel Laboratories) at 130 μg/ml in buffer B for 1 h at 37°C followed by four successive soaks in buffer B at 23°C, or they were incubated with biotinylated goat anti-rabbit IgG for 1 h at 37°C, given four 15-min soaks in buffer B at 23°C, and labeled with fluorescein avidin DCS (Vector Laboratories, Inc.) at 50 μg/ml for 40 min at 37°C. Coverslips were mounted for viewing as described in the second section of Materials and Methods.

Electrophoresis Conditions: An electrophoresis chamber was designed for use with 22 × 30-mm No. 1 glass coverslips based on the design of Poo et al. (28). Briefly, a 400-μm-deep trough was machined into a 1″ × 3″ × ¼″ plexiglas plate that would hold the coverslip. Wells for immersion of agar-bridge electrodes were machined at each end of the trough. After insertion of the coverslip, cell-side-up into the trough, a glass plate was sealed to the surface of the plexiglas, conversing the trough, with lilicone grease. The chamber was subsequently filled with Medium 199 supplemented with 10 mM HEPES by capillary movement of buffer from one well to the other through the 22-mm × 200-μm × 30-mm-long tunnel defined by the side of the coverslip plated with cells, the edges of the trough, and the bottom of the glass plate sealed to the chamber top. Both applied voltage and current were monitored, and in all experiments reported in this paper, a field strength of 10 V/cm was used. In many of the experiments, standard electrophoresis conditions were used. These are defined as exposure of the coverslip to a 10 V/cm field for 1 h at 22°C ambient temperature.

Microscopy: All observation and microscopy of cells were done using a Nikon Optiphot epi-fluorescence microscope (Nikon Inc., Garden City, NY). Color slides were taken with Kodak Ektachrome push-processed with E6 chemicals to ASA 6400; black and white prints from these slides were printed using Kodak Technical Pan film internegatives. Direct black and white negatives were obtained using Kodak Tri-X film push-processed at ASA 3200 in Kodak D-19 developer.

Cell Scoring for LDL-RC Asymmetry and Cell Width: Cells were scored for percent asymmetry (%A) as follows. A coverslip was sequentially scanned using a procedure to prevent duplicate scoring of any given cell. If the density of LDL-RC, as determined by the fluorescence pattern using one of the labeling protocols described above, was higher on the cathodal side of the cell (the side of the cell nearest to the negative electrode) than the anodal side, then this cell was scored as asymmetric. Then the %A of a population of cells is defined as the number of asymmetric cells per total number of cells examined. This is equivalent to the definition used by others (28, 29, 30), since no cells showed a distribution that had higher LDL-RC density on the anodal side.

The distribution of cell widths was determined by scanning a coverslip of cells as above and measuring the longest dimension in a specified direction of each cell using a grid-containing monocular.

RESULTS

Redistribution of LDL-Rs on GM2408A and GM3348 Cells

When GM3348 or GM2408A cells are cooled to 4°C and have their LDL-Rs complexed with the highly fluorescent dil(3)-LDL, the receptor complexes appear as bright dots. Indirect immunofluorescent labeling, using an antibody directed against unlabeled receptor-bound LDL followed by the highly fluorescent biotin-avidin labeling system, can also be used to identify the receptor complexes with equivalent results. On GM2408A cells, these dots appear punctate and are randomly distributed over the dorsal surface. On GM3348 cells, the dots often appear brighter, indicating the complexes are clustered in groups of 3–4, and occasionally clusters are arranged in linear arrays, especially over the nucleus (6, 24, 31). Although the density of LDL-Rs is low, only several per square micrometer, individual receptors are optically detectable using fluorescence techniques because they are complexed with an LDL particle, and each LDL particle is associated with a high number of fluorescent molecules.

Exposure of GM2408A cells to a constant electric field of 10 V/cm that is oriented parallel to the cell surface alters the initially random topographical distribution of unliganded LDL-R's. As shown in Fig. 1 *a*, exposure to this field for a duration of 1 h produces an unambiguous asymmetry: LDL-Rs, fluorescence labeled after field exposure, are highly concentrated on the side of the cell exposed to the lower potential, the cathodal (−) side. For comparison, a phase micrograph of the same cell is shown is Fig. 1 *b*. Note that although we are photographing the LDL-RC in fluorescence, the redistribution occurred for the unliganded LDL-R, since the cells were postfield fixed and subsequently labeled.

We have done several experiments to see whether field exposure has caused any cellular changes in morphology that might accompany or be responsible for the redistribution of LDL-Rs that we observe. In the double label experiment shown in Fig. 1, we have compared the generated LDL-R asymmetry with the topographic distribution of F-actin, by use of the F-actin-specific fluorescence-labeled probe NBD-phallacidin (Fig. 1 *c*). The distribution of this major component of the cytoskeleton is not asymmetric. It appears identical to what is observed in control cells not exposed to the field. In another experiment, low-power phase micrographs of fields of cells on a coverslip were taken before and after exposure to a 10 V/cm electric field for 1 h. Comparison of the two micrographs showed that the relative positions of every cell within a given field had not changed (data not shown). Also, time lapse photomicrographs of individual cells taken during exposure to the field showed only small shifts (<2 μm) in the cell periphery during a 1-h exposure. Finally, scoring cells as to whether the nuclear hump was located nearer the cathodal or anodal edge of the cell showed no preferential orientation after exposure to the field. Hence, LDL-R redistribution is not an artifact caused by changes in cell morphology.

By postfield indirect immunofluorescence labeling using an antibody directed against the coat protein clathrin, we were able to investigate the association of the LDL-R with coated pits. As shown in Fig. 2, exposure of GM2408A cells to an electric field under conditions that induce unambiguous redistribution of LDL-R did not result in any asymmetric distribution of coated structures. Two symmetric populations remained: the internal coated vesicles visible as a slight halo around the nucleus, and the large number of dots (coated pits) over the rest of the cell's image that are occasionally seen arranged in linear arrays. We can conclude that there was little or no redistribution of coated pits induced by field application. No movement of coated pits was observed in similar experiments with GM3348 cells (data not shown).

In our initial experiments with the normal fibroblast GM3348, electrophoresis-induced asymmetric redistribution of LDL-R appeared inhibited, relative to GM2408A cells, but not absent. To quantitate the difference between the normal and internalization-defective cells, we adopted the following scheme: Coverslips of each cell type, under identical conditions of cell growth, buffers, duration in field, etc., were scored by counting the number of cells that exhibited a difference in LDL-R density, detectable by eye (see next section of Results),

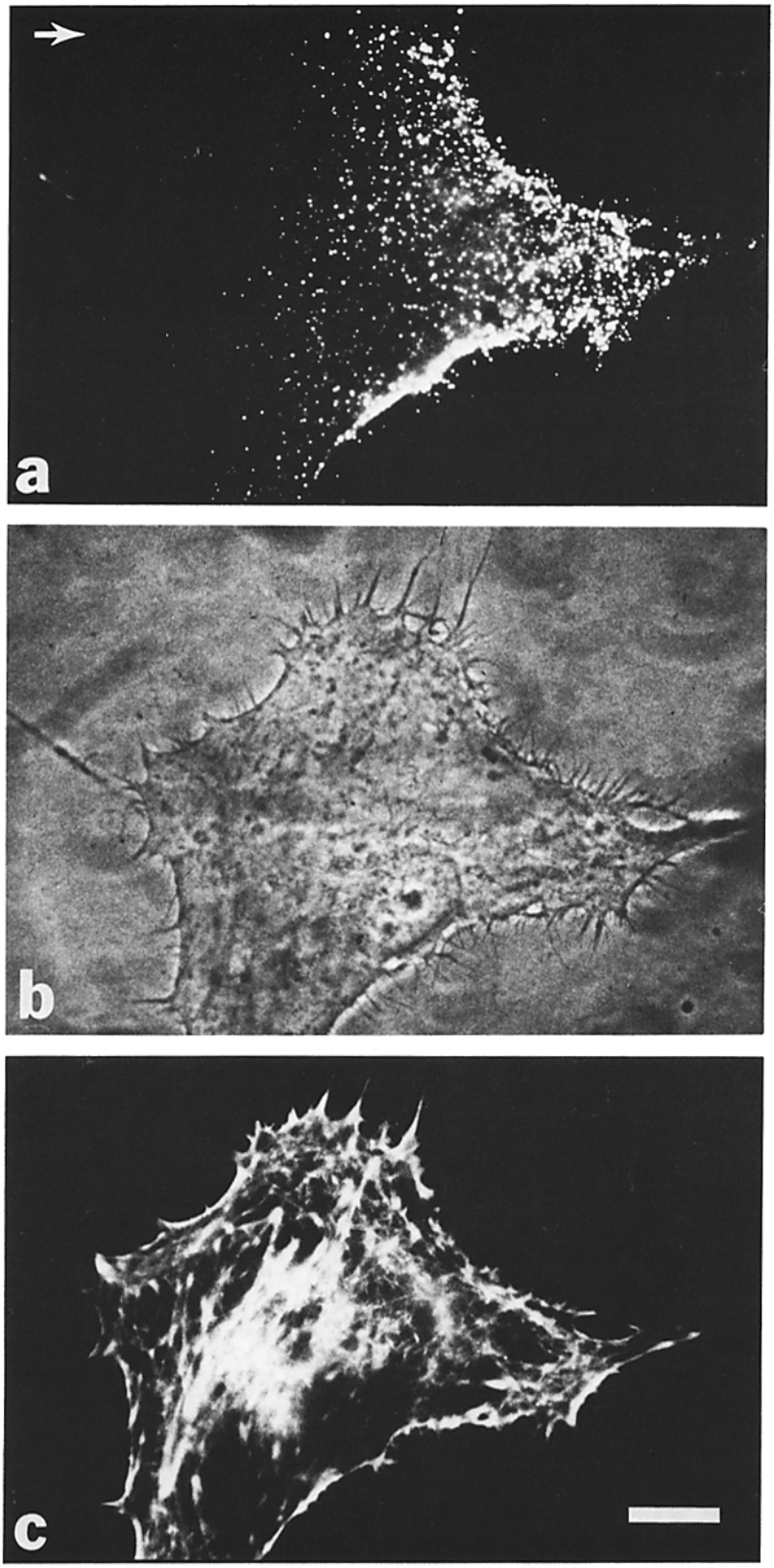

FIGURE 1 LDL-R distribution and actin cytoskeleton in a GM2408A human fibroblast exposed for 1 h to an electric field of 10 V/cm. This cell was postfield double-labeled using indirect immunofluorescence against unlabeled LDL and NBD-phallacidin as detailed in the Materials and Methods section. The applied electric field was oriented in the direction of the arrow in the figure. Bar, 12 μm. (a) Fluorescence micrograph of labeled LDL-Rs. Cells were incubated sequentially with LDL, rabbit anti-human beta lipoprotein, biotinylated goat anti-rabbit IgG, and rhodamine-labeled avidin D. (*b*) Phase micrograph showing boundaries of the cell. (c) Fluorescence micrograph of actin cytoskeleton labeled with NBD-phallacidin.

between their farthest upfield and farthest downfield edges. For each cell type, this number divided by the total number of cells on the coverslip being scored gave the percentage of cells showing an asymmetric distribution (%A). In Table I, we show the combined results (mean %A ± SEM) of three of these back-to-back experiments. Ignoring any morphological subclassifications of cells and scoring all equally, ~20% of the normal cells showed asymmetry compared to >80% of the internalization-defective cells. Closer examination according to cell morphology (flat, spindle-shaped, and elongated) as indicated in the table shows that each morphological subclass of GM2408A cells had a larger %A than did its counterpart in the GM3348 cells.

We tested the ability of neuraminidase treatment before

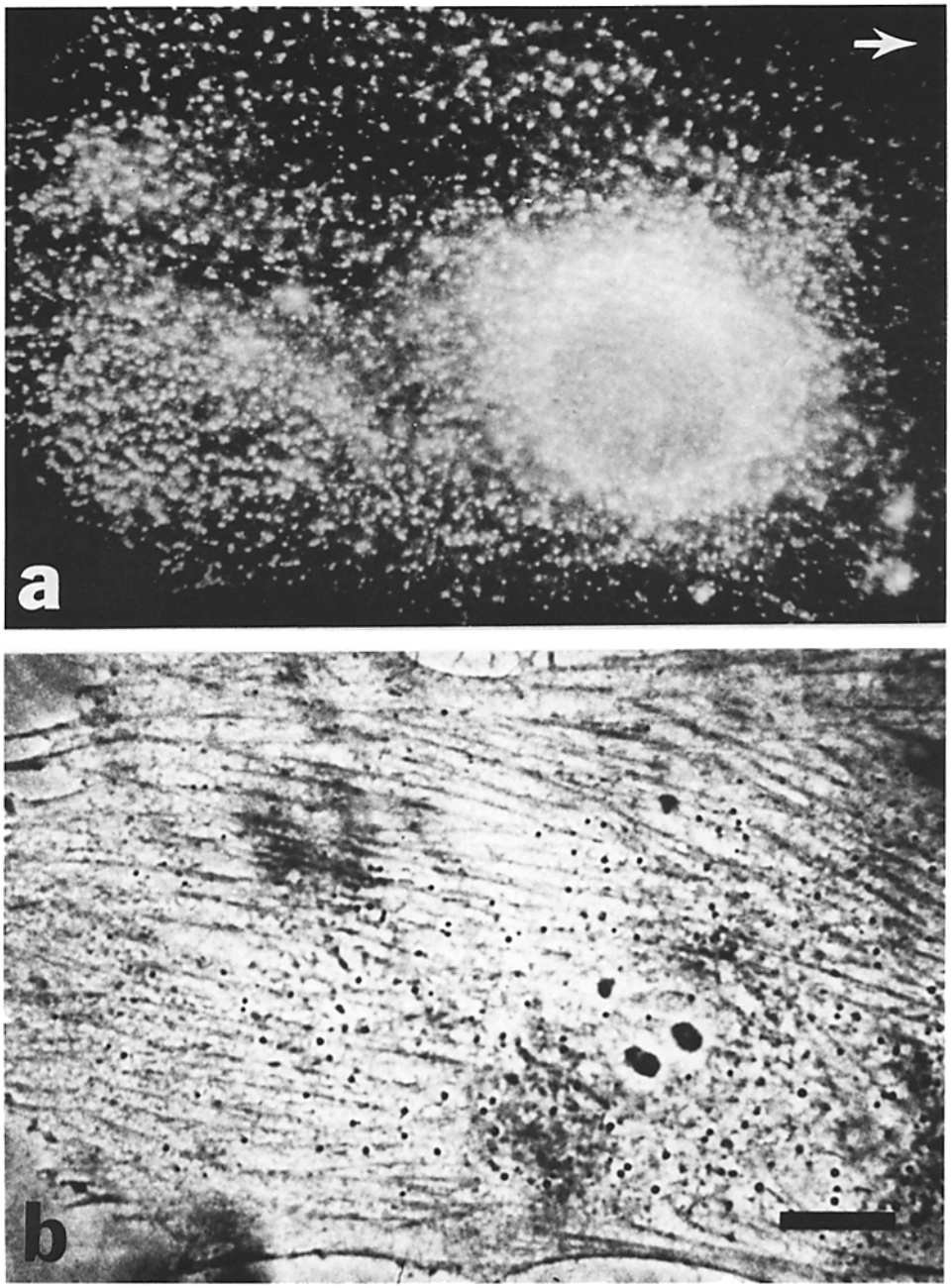

FIGURE 2 The distribution of coated pits and coated vesicles in a GM2408A fibroblast after a 1-h exposure to a 10 V/cm electric field. Cells were postfield fixed, extracted, and labeled with rabbit anti-clathrin antibody (the generous gift of M. S. Brown, J. L. Goldstein, and R. G. W. Anderson) followed by rhodamine-labeled goat anti-rabbit IgG. The applied field direction is indicated by the arrow. Bar, 12 μm. (*a*) Rhodamine fluorescence micrograph. (*b*) Phase micrograph, same field of view as in *a*.

TABLE I. *Percent Asymmetry (%A): Effect of Cell Type and Morphology*

		Spindle*		Elongated*	
	Flat	>45°	<45°	>45°	<45°
GM2408A	(93 ± 7)%	(89 ± 4)%	(66 ± 15)%	(61 ± 17)%	(25 ± 25)
GM3348	(34 ± 16)%	(33 ± 29)%	(10 ± 5)%	(18 ± 16)%	(0 ± 0)%

* The angle between the long axis of the cell and the field direction was used to subclassify these cells (<45° or >45°).

field application to reverse the direction of the LDL-R movement on GM2408A cells, since reversal by this procedure for reducing the cell surface charge has been observed for other membrane components (23). Pretreatment of the cells with 0.1 U/ml of this enzyme for 1 h at 37°C did not reverse the direction of LDL-R electrophoresis.

Postfield Relaxation on GM2408A

As shown in Fig. 3, the percentage of GM2408A cells showing an asymmetric LDL-R distribution increased, at short exposure times, with the duration of exposure to the field. At 22°C, %A reached a plateau of >80% at ~60 min. For a 60-min duration of electrophoresis, in most cells the LDL-R distribution appeared as a gradient: as shown in Fig. 4, there was a monotonic decrease in density of receptors as the cell was traversed from cathodal to anodal edges. Since each fluorescent dot represents an average number of LDL-Rs (1–3 on GM2408A; see reference 20), we could directly

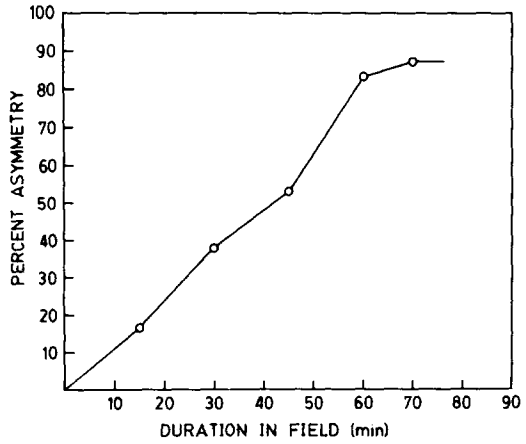

FIGURE 3 The percentage of GM2408A cells showing an asymmetric distribution of LDL-R (%A) as a function of the exposure time to a 10 V/cm electric field at 22°C.

quantitate the receptor density gradient from analysis of an enlarged fluorescence photomicrograph. The result of such a measurement is shown in Fig. 5. There is an exponential decay of density with traversal from the cathodal edge. This experimental distribution is consistent with what is expected if electrophoresis of the receptor is in equilibrium with Brownian motion (back diffusion). Modeling the cell as a one-dimensional system, then in equilibrium, the diffusive flux must equal the electrophoretic flux:

$$\mu E C_E(x) = -D[\partial C_E(x)/\partial x], \tag{1}$$

where $C_E(x)$ is density of LDL-R per unit distance (particles/cm^2), D is diffusion coefficient of the LDL-R, μ is electrophoretic mobility of the LDL-R, and E is electric field. The solution of this equation under the boundary conditions of an initial uniform density (C_0) of receptors on the cell of width L with impermeable boundaries at $x = 0, L$ (i.e., $\partial C_E(x)/\partial x = 0$ at $x = 0, L$) gives

$$C_E(x) = [\beta C_0 L/(1 - e^{-\beta L})]e^{-\beta x}, \tag{2}$$

where $\beta = \mu E/D$. Hence, the simple model of back diffusion in equilibrium with electrophoresis can explain the observed exponential distribution. The constant β can be empirically determined from the slope of the curve in Fig. 5. For this data, $\beta = 0.325/\mu$m; similar measurements on several other cells showed similar decay constants, although the distributions sometimes showed a sum of an exponential and a small constant background. This constant background was probably not the result of nonspecific binding of the fluorescent probe, since postfield labeling of the mutant human fibroblast cell line GM2000, which lacks a functional LDL-R binding site, showed virtually no surface fluorescence. The average value of β for these electrophoresis conditions of GM2408A cells was $0.32/\mu$m. Note that if diffusive processes were not present and receptors moved only electrophoretically, then the receptors would move with uniform velocity until they reached the edge of the cell where they would be trapped. Assuming equal electrophoretic mobility for all receptors, the distribution at any duration of exposure would not be exponential.

Although the one-dimensional model is obviously a simplification and the complicated geometry of these cells does not allow an easy mathematical modeling of the situation, it can help us estimate the diffusion coefficient of the unliganded LDL-R by analysis of a postfield relaxation experiment. A series of coverslips plated with GM2408A cells were exposed to the standard electrophoresis conditions of 10 V/cm for 1 h at 22°C. Each coverslip was then removed from the chamber and incubated for a different length of time, at either 37°, 22°, or 10°C, before fixation and labeling with dil(3)-LDL. The coverslip was then scored for %A. As described in the Materials and Methods section, cells were scored as asymmetric if the density of receptors was higher on the cathodal as opposed to the anodal edge. The combined results of four experiments are shown in Fig. 6. Data are shown only for cells of flat morphology, since virtually all cells of this type start off the relaxation with asymmetric distributions (see Table I), and the cell widths (see below) were better defined for these cells. There is a temperature-dependent relaxation of %A with increasing incubation time. The time-dependent relaxation is understandable because the cells have different widths—wider cells will require a longer amount of time for diffusive processes to relax the concentration gradients to the point at which the concentration difference between the cathodal and anodal edge is below the eye's detectability. (In separate experiments, we observed that labeling the LDL-R with dil(3)-LDL immediately after electric field exposure inhibited the relaxation [data not shown].)

In the one-dimensional model, all cells start the relaxation period with the equilibrium concentration distribution in Eq. (2) above except that the L is different for each cell. β is empirically measured as described and should be independent of L. Then the solution to the time-dependent diffusion equation, which describes the time evolution of the concentration distribution, is (32)

$$C(x, t) = 1/L \int_0^L C_E(x')dx' + 2/L \sum_{n=1}^{\infty} e^{-Dn^2\pi^2 t/L^2} \cdot \cos(n\pi x/L) \int_0^L C_E(x') \cos(n\pi x'/L)dx'. \tag{3}$$

Evaluation of the integrals using $C_e(x')$ from Eq. (2) gives

$$C(x, t) = C_0 + 2C_0[\gamma^2/(1 - e^{-\gamma\pi})] \cdot \sum_{n=1}^{\infty} \{e^{-Dn2\pi^2 t/L^2}\cos(n\pi x/L) \cdot [[1 + (-1)^{n+1}e^{-\gamma\pi}]/(\gamma^2 + \pi^2)]\}, \tag{4}$$

where $\gamma = L\beta/\pi$. Now the concentration difference we are evaluating in scoring a given cell as having an asymmetric distribution of LDL-RC is

$$\Delta = \text{Fractional concentration difference between edges} = |C(0, t) - C(L, t)|/C_0. \tag{5}$$

Evaluation of this expression gives

$$\Delta = 4\gamma^2[(1 + e^{-\gamma\pi})/(1 - e^{-\gamma\pi})] \cdot \sum_{n=1,\text{odd}}^{\infty}, (e^{-Dn^2\pi^2 t/L^2})/(\gamma^2 + n_2). \tag{6}$$

This is a rapidly converging serics with, for our conditions, the second term $<10^{-9}$ of the first term. Hence for our purposes, it is necessary only to include the first term, and we can reduce the expression for Δ to

$$\Delta = 4\gamma^2[(1 + e^{-\gamma\pi})/(1 - e^{-\gamma\pi})][e^{-D\pi^2 t/L^2}/(1 + \gamma^2)] \tag{7}$$

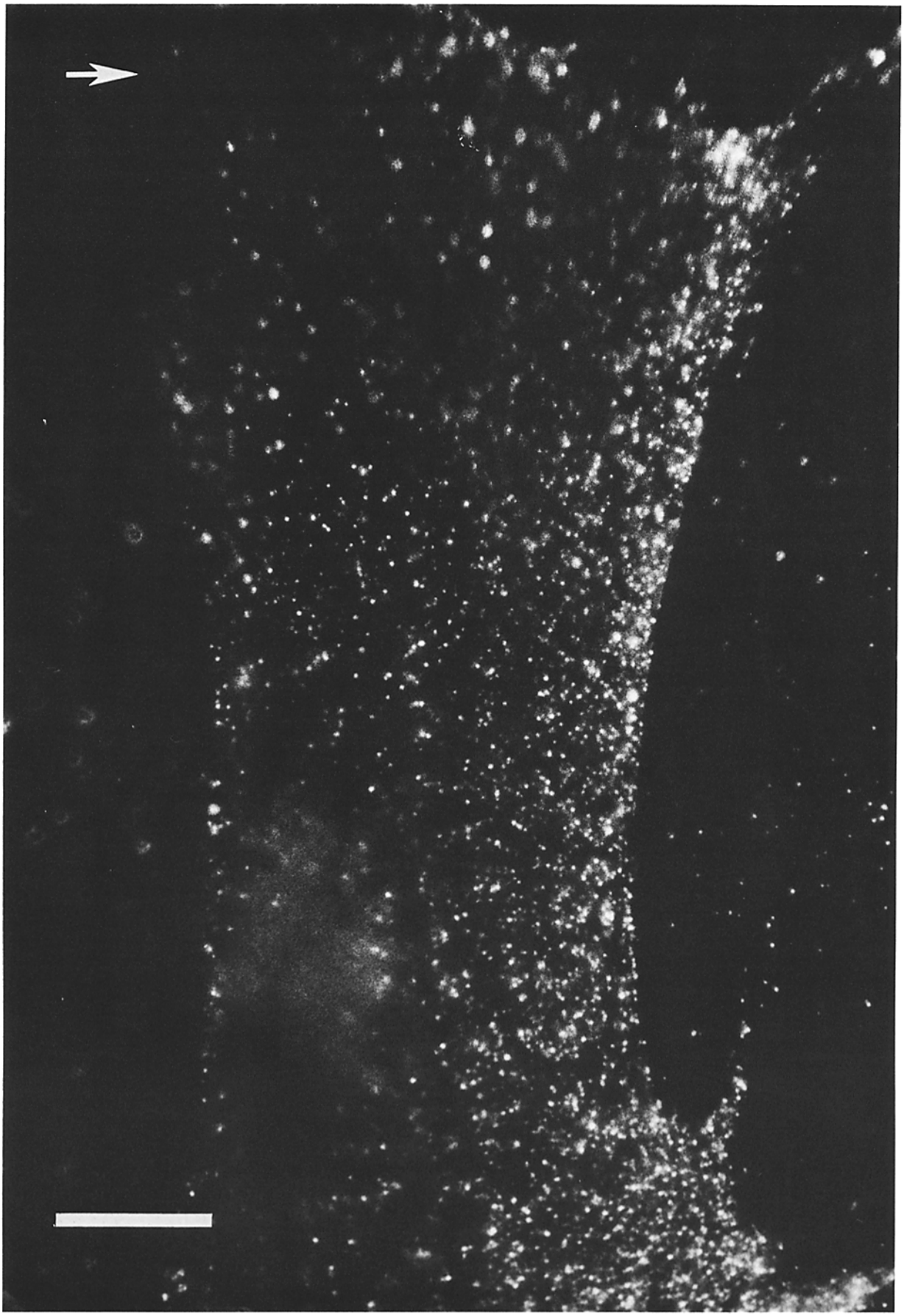

FIGURE 4 The exponential decrease in LDL-R surface concentration with increasing distance from the cathodal edge of a rectangularly shaped GM2408A fibroblast postfield labeled with dil(3)-LDL after exposure to a 10 V/cm field for 1 h at 22°C. This is a fluorescence micrograph of dil(3)-LDL distribution. Bar, 12 μm. The direction of applied field was perpendicular to the long edge of the cell.

If we define Δ_{min} as the estimated minimum fractional difference in dot density that the eye can detect, then for any specified relaxation time (t_{rel}), there will be a corresponding maximum width L_{max} such that for all cells, $L < L_{max}$ and $\Delta < \Delta_{min}$. Hence, they are scored as symmetric. We have measured the empirical distributions of cell widths for flat cells in the GM2408A cultures—they are nearly Gaussian—and from this distribution $\rho(L)$, we can theoretically determine the percentage of cells still showing an asymmetric distribution at t_{rel} (i.e., the %A) as

$$\%A(t_{rel}) = 1 - \int_0^{L_{max}} (t_{rel}, D, \beta, \Delta_{min})\rho(L)dL, \quad (8)$$

where $\rho(L)$ is distribution of cell widths (normalized). Note that $\%A(t_{rel})$ has only two undetermined parameters (D, Δ_{min}) since β and $\rho(L)$ are determined experimentally. For a fixed value of Δ_{min}, determination of the best value of D that produces an $A\%(t_{rel})$ closely matching the experimental distribution allows an estimate of the diffusion coefficient for the unliganded receptor. Although Δ_{min} is a variable parameter in this model and must be chosen, note that an overly conservative value for Δ_{min} will underestimate D. So we can, by choosing such an overly conservative estimate, use our model to obtain a lower bound estimate of D. The human eye can easily detect a fractional concentration difference of 50% (at these concentration ranges), but empirically we have found that it is difficult to discriminate <20% changes. Taking the conservative estimate of $\Delta_{min} = 0.5$ and using the measured β and $\rho(L)$, we have generated theoretical %A relaxation curves by computer, as shown in Fig. 6. The only difference in the computation of the three different curves shown is the value of D used, which was chosen so that the curves closely fit the experimental data; the functional shape of the curves matches the data very well. The values of D used are best-fit lower-bound estimates for D of the unliganded LDL-R and are shown in Table II; also shown are the extreme values obtained if one used $\Delta_{min} = 0.1$ and 1.0.

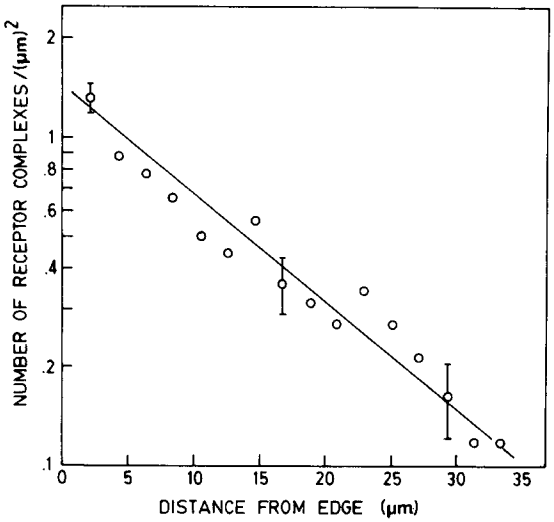

FIGURE 5 A semilogarithmic plot of LDL-R surface concentration versus linear distance from the cathodal edge of the cell. This distribution was determined as outlined in the text, using an enlargement of a micrograph similar to the one shown in Fig. 4.

DISCUSSION

We have exploited the ability of an applied electric field to induce an asymmetric distribution of LDL-R on cultured human fibroblasts to study the lateral mobility of the unliganded receptor and its interaction with coated membranes. Our central result is that the LDL-R on the internalization-deficient mutant cell line GM2408A redistributes rapidly without concomitant change in coated pit topology or gross cellular morphology. Examination of the time-course of the redistribution shows that the postfield lateral diffusion of this membrane component is rapid.

We have not proven that the electric field–induced redistribution of the LDL-R is actually surface electrophoresis, but the several control experiments we have done do rule out major cell ultrastructural changes, cell movement, and internal flows. The observation that many types of membrane components can be electrophoretically redistributed (for a review, see reference 13) suggests that the simplest explanation

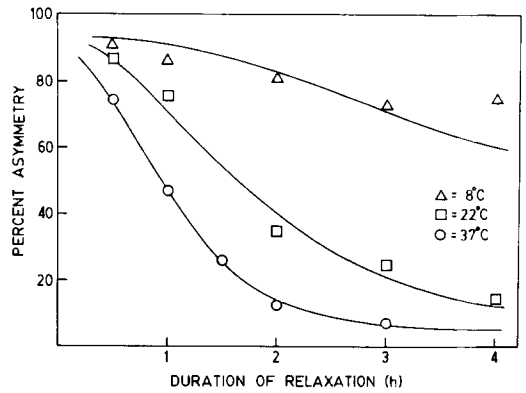

FIGURE 6 Relaxation in the percentage of flat GM2408A fibroblasts showing an asymmetric distribution of LDL-R (%A) with increasing incubation time after field exposure. The data points represent the combined data from 2–4 experiments at each temperature. The solid curves were generated from the one-dimensional relaxation model as described in the text. The diffusion coefficients that correspond to these curves are shown in Table II.

TABLE II. *Diffusion Coefficients of the Liganded and Unliganded LDL-R*

Conditions	Method	D	Temperature
LDL-R (unliganded)	Postfield relaxation	2.0×10^{-9} (0.9–2.5)*	37
LDR (unliganded)	Postfield relaxation	1.1×10^{-9} (0.5–1.5)*	22
LDL-R (unliganded)	Postfield relaxation	3.5×10^{-10} (1.6–4.0)*	8
LDL-RC (liganded)	Photobleaching	$<10^{-11}$‡	10
LDL-RC (liganded)	Photobleaching	$(0.5–1.5) \times 10^{-11}$‡	22
LDL-RC (liganded, bleb)	Video observation	$(2–4) \times 10^{-9}$‡	22

* The range of values indicated in the parentheses shows the extreme values for the mantissa of D when $0.1 \leq \Delta_{min} \leq 1.0$.
‡ From Barak and Webb (13).

for our observations is that the LDL-Rs have been redistributed by forces acting on the receptor on the cell surface.

The inhibition of generated asymmetry in GM3348 cells is consistent with the idea that there is a continuous recycling of LDL-R via coated vesicles even in the absence of LDL binding. The average lifetime of a coated pit at 22°C is about 5 min (10, 33), so that assuming the recycling time is long compared with this value, the receptor is actually on the surface for only a fraction of the total electrophoresis time. Hence, although an asymmetric distribution may still be observed if exposure to the field is long enough (or strong enough) in comparison to the GM2408A cells, for any given condition we would expect a smaller effect. This is consistent with our observation of a smaller value of %A for GM3348 in the GM2408A/GM3348 back-to-back experiments, while we could still induce some asymmetry in the GM3348 cells. Alternative explanations for these results include the possibility that on different cells, different proportions of LDL-Rs are undergoing continual recycling, hence cells with high values of free receptor might show asymmetry. However, the immunofluorescence studies of recycling of LDL-R in the presence of monensin (34) seem to rule out this possibility—a difference between subpopulations of cells was not reported—although they suggest that ~50% of the LDL-R on the normal cells are not undergoing continuous recycling. It is possible that only 50% of the LDL-R are available for redistribution in the electric field, hence the smaller %A, but this would imply that a constant baseline density of receptors would always be observed on the electrophoresed cells, even on the anodal side, but this was not observed; occasionally GM3348 cells showed areas of surface devoid of any receptors (always on the anodal edge).

Our lower bound estimate for the lateral diffusion coefficient of the postfield unliganded LDL-R on GM2408A cells obtained by scoring large numbers of cells for asymmetry after a particular postfield relaxation period implies that this membrane component is very mobile compared with the LDL-bound LDL-RC on the normal cell surface. Postfield relaxation estimates of D have now been carried out for several types of membrane components. For the lipid probe dil(3), relaxation experiments by Poo (23) have shown that on immature *Xenopus* myocytes, $D = 3 \times 10^{-8}$ cm^2/s, about what has been measured by photobleaching methods on a variety of cells (see reference 35 for a review). Experiments on *Xenopus* cells of relaxation of asymmetry in functional acetylcholine receptors induced by local application of alpha-bungarotoxin (36), has given $D = 2 \times 10^{-9}$ cm^2/s. However, this diffusivity could not be measured by the electrophoresis-relaxation method because, in this system, electric field application induced receptor aggregates that were immobile. Fluorescence photobleaching recovery measurements on normal cell surface of cultured rat myotubes of the fluorescent alpha-bungarotoxin-labeled acetylcholine receptor (37) yield values about 10-fold smaller than that measured on *Xenopus* myocytes. It is not clear at the present time if this difference reflects a species variation or an inconsistency of techniques (Axelrod, D, and M.-m. Poo, personal communication).

Zagyanksy and Jarad (29, 30) have done both fluorescence photobleaching recovery and electrophoresis induced redistribution relaxation on several lectin receptors on cultured cells and found that lectin-labeled receptors show highly restricted lateral mobility by fluorescence photobleaching recovery, undergo internalization, and cannot be induced to redistribute asymmetrically by an electric field. In contrast, unlabeled receptors can be electroredistributed and show rapid relaxation of asymmetry consistent with fast lateral diffusion.

How can we explain the fast diffusion of the postfield unliganded LDL-R compared with fluorescence photobleaching recovery measurements of the LDL-RC? One obvious possibility is that, for this system, the application of an electric field has reorganized the plasma membrane so as to change protein interactions. The postfield ligand effects cited above seem to be consistent with field-induced release of constraints on protein diffusion that can sometimes be restored by ligand binding. The diffusion coefficient of LDL-RC on membrane blebs, where constraints have been released, is comparable to the effective postfield values for LDL-R on GM2408A cells. Field application to preliganded LDL-RC on GM2408A cells enhanced the LDL internalization rate enough to prevent electric-field induced redistribution of LDL-RC in our preliminary experiments. We do not know if the prefield unliganded LDL-R also exhibits rapid diffusion.

An alternative possibility is that binding of the large LDL particle to the cell receptor causes a constraint on the diffusibility of the LDL-R. This constraint would probably not be the result of the hydrodynamic drag exerted on the LDL particle by the extracellular bathing solution as the LDL-RC was undergoing Brownian motion because measurements of the LDL-RC on cell membrane blebs show rapid diffusion. However, as has been postulated for the inhibition of stearoylated-dextran-model-receptor diffusion of 3T3 plasma membranes, the LDL particle may, due to its specific chemical properties, interact with immobilized components of the extracellular matrix or lamina, and hence show reduced mobility. Likewise, the lateral mobility may be impeded as a result of nonspecific viscous drag exerted on the large LDL particle by this extracellular matrix. At least one component of the extracellular matrix, fibronectin, is known to be immobilized on the plasma membrane surface (38). Also, the exoskeleton may be depleted from cell surface blebs, explaining the observed rapid lateral diffusion of the LDL-RC in that system. Our observation that postfield labeling of the asymmetric distribution of LDL-Rs inhibits relaxation (and causes some internalization) is also consistent with the idea that LDL binding to the LDL-R sterically or specifically hinders LDL-RC lateral mobility. Postfield immobilization by ligand binding has also been observed for lectin receptors (29).

We hope that further investigation of the differences between the mobility and internalization of the LDL-R with and without and before, during, and after electrophoresis will provide some understanding of the controlling mechanisms. Video fluorescence microscopy tracking of individual LDL-RCs during diffusion and electromigration is currently in progress in our laboratory with that objective (39).

This work was supported by National Science Foundation grant No. 80-07634 and was aided by facilities at Cornell supported by National Science Foundation grant No. DMR-79-24008-A03 and National Institutes of Health grants GM-27533-03 and CA 14454. D. W. Tank also held a National Institutes of Health predoctoral traineeship.

Received for publication 26 January 1983, and in revised form 21 January 85.

REFERENCES

1. Goldstein, J. L., and M. S. Brown. 1977. Low density lipoprotein pathway and its relationship to atherosclerosis. *Ann. Rev. Biochem.* 46:897–930.

2. Orci, L., J. L. Carpeitier, A. Perrelet, R. G. Anderson, J. L. Goldstein, and M. S. Brown. 1978. Occurrence of low density lipoprotein receptors within large pits on the surface of human fibroblasts as demonstrated by freeze-etching. *Exp. Cell Res.* 113:1–13.
3. Goldstein, J. L., R. G. Anderson, and M. S. Brown. 1979. Coated pits, coated vesicles, and receptor mediated endocytosis. *Nature* (*Lond.*). 279:679–685.
4. Jarett, L., and R. M. Smith. 1974. Electron microscopic demonstration of insulin receptors on adipocyte plasma-membranes utilizing a ferritin-insulin conjugate. *J. Biol. Chem.* 249:7024–7031.
5. McKanna, J. A., H. T. Haigler, and S. Cohen. 1979. Hormone receptor topology and dynamics. Morphological analysis using ferritin-labeled epidermal growth factor. *Proc. Natl. Acad. Sci. USA.* 76:5689–5693.
6. Anderson, R. G., E. Vasile, R. J. Mello, M. S. Brown, and J. L. Goldstein. 1978. Immunocytochemical visualization of coated pits and vesicles in human fibroblasts: relation to low density lipoprotein receptor distribution. *Cell.* 15:919–933.
7. Brown, M. S., and J. L. Goldstein. 1979. Receptor-mediated endocytosis: insights from the lipoprotein receptor system. *Proc. Natl. Acad. Sci. USA.* 76:3330–3337.
8. Schlessinger, J., Y. Shechter, P. Cuatrecasas, M. C. Willingham, and I. Pastan. 1978. Quantitative determination of the lateral diffusion coefficients of the hormone-receptor complexes of insulin and epidermal growth factor on the plasma membrane of cultured fibroblasts. *Proc. Natl. Acad. Sci. USA.* 75:5353–5357.
9. Schlessinger, J., Y. Shechter, M. C. Willingham, and I. Pastan. 1978. Direct visualization of the binding, aggregation, and internalization of insulin and epidermal growth factor on fibroblastic cells. *Proc. Natl. Acad. Sci. USA.* 75:2135–2139.
10. Brown, M. S., and J. L. Goldstein. 1976. Analysis of a mutant strain of human fibroblasts with a defect in the internalization of receptor-bound low density lipoprotein. *Cell.* 9:663–674.
11. Goldstein, J. L., and M. S. Brown. 1977. Genetics of the LDL receptor: evidence that the mutations affecting binding and internalization are allelic. *Cell.* 12:629–641.
12. Barak, L. S., and W. W. Webb. 1981. Molecular motion of individual LDL molecules on cell membranes. *Biophys. J.* 33(2, Pt. 2):74*a* (Abstr.)
13. Barak, L. S., and W. W. Webb. 1982. Diffusion of low density lipoprotein-receptor complex on human fibroblasts. *J. Cell. Biol.* 95:846–852.
14. Wu, E.-S., P. S. Low, and W. W. Webb. 1981. Lateral diffusion of glycophorin reconstituted into phospholipid multibilayers. *Biophys. J.* 33(2, Pt. 2):109*a*. (Abstr.)
15. Tank, D. W., E.-S. Uw, P. R. Meers, and W. W. Webb. 1982. Lateral diffusion of gramicidin C in phospholipid multibilayers: effects of cholesterol and high gramicidin concentration. *Biophys. J.* 40:129–135.
16. Tank, D. W., E.-S. Wu, and W. W. Webb. 1982. Enhanced molecular diffusibility in muscle membrane blebs: release of lateral constraints. *J. Cell Biol.* 92:207–212.
17. Wu, E.-S., D. W. Tank, and W. W. Webb. 1982. Unconstrained lateral diffusion of concanavalin A receptors on bulbous lymphocytes. *Proc. Natl. Acad. Sci. USA.* 79:4962–4966.
18. Axelrod, D., D. E. Koppel, J. Schlessinger, E. Elson, and W. W. Webb. 1976. Mobility measurement by analysis of fluorescence photobleaching recovery kinetics. *Biophys. J.* 16:1055–1069.
19. Smith, A. A., and H. M. McConnel. 1978. Determination of molecular motion in membranes using periodic pattern photobleaching. *Proc. Natl. Acad. Sci. USA.* 75:2759–2763.
20. Jaffe, L. F. 1977. Electrophoresis along cell membranes. Nature (*Lond.*). 265:600–602.
21. Poo, M.-m., and K. R. Robinson. 1977. Electrophoresis of concanavalin A receptors along embryonic muscle cell membrane. Nature (*Lond.*). 265:602–605.
22. McLaughlin, S., and M.-m. Poo. 1981. The role of electro-osmosis in the electric-field-induced movement of charged macromolecules on the surfaces of cells. *Biophys. J.* 34:85–93.
23. Poo, M.-m. 1981. In situ electrophoresis of membrane components. *Annu. Rev. Biophys. Bioeng.* 10:245–276.
24. Barak, L. S., and W. W. Webb. 1981. Fluorescent low density lipoprotein for observation of dynamics of individual receptor complexes on cultured human fibroblasts. *J. Cell Biol.* 90:595–604.
25. Brown, M. S., S. E. Dana, and J. L. Goldstein. 1973. Regulation of 3-hydroxy-3-methylglutaryl coenzyme A reductase activity in human fibroblasts by lipoproteins. *Proc. Natl. Acad. Sci. USA.* 70:2162–2166.
26. Albutt, E. C. 1966. *J. Med. Lab. Technol.* 23:61–82.
27. Barak, L. S., and R. R. Yocum. 1981. 7-Nitrobenz-2-oxa-1,3,diazole-phallacidin. Synthesis of a fluorescent actin probe. *Anal. Biochem.* 110:31–38.
28. Poo, M.-m., W.-j. H. Poo, and J. W. Lam. 1978. Lateral electrophoresis and diffusion of concanavalin A receptors in the membrane of embryonic muscle cell. *J. Cell Biol.* 76:483–501.
29. Zagyansky, Y. A. and S. Jarad. 1979. Does lectin-receptor complex formation produce zones of restricted mobility within the membrane? *Nature* (*Lond.*). 280:591–593.
30. Zagyansky, Y., and S. Jarad. 1981. The effect of amphotericin B on lectin-induced aggregation of cell surface receptors. *Exp. Cell Res.* 132:387–397.
31. Anderson, R. G. W., J. L. Goldstein, and M. S. Brown. 1980. Fluorescence visualization of receptor-bound low density lipoprotein in human fibroblasts. *J. Recept. Res.* 1:17–39.
32. Crank, J. 1956. The Mathematics of Diffusion. Oxford University Press, Oxford, UK.
33. Goldstein, J. L., S. K. Basu, G. Y. Brmschede, and M. S. Brown. 1976. Release of low density lipoprotein from its cell-surface receptor by sulfated glycosaminoglycans. *Cell.* 7:85–95.
34. Basu, S. K., J. L. Goldstein, R. G. W. Anderson, and M. S. Brown. 1981. Monensin interrupts the recycling of low density lipoprotein receptors in human fibroblasts. *Cell.* 24:493–502.
35. Cherry, R. J. 1979. Rotational and lateral diffusion of membrane proteins. *Biochim. Biophys. Acta.* 559:298–327.
36. Young, S. H., and M.-m. Poo. 1982. Lateral diffusion of ligand-free acetylcholine receptors in vivo measured by local inactivation recovery. *Biophys. J.* 37(2, Pt. 2)309*a*. (Abstr.)
37. Axelrod, D., P. Ravdin, D. E. Koppel, J. Schlessinger, W. W. Webb, E. L. Elson, and T. R. Podleski. 1976. Lateral motion of fluorescently labeled acetylcholine receptors in membranes of developing muscle fibers. *Proc. Natl. Acad. Sci. USA.* 73:4594–4598.
38. Schlessinger, J., L. S. Barak, G. C. Hammes, K. M. Yamada, I. Pastan, W. W. Webb, and E. L. Elson. 1977. Mobility and distribution of a cell surface glycoprotein and its interaction with other membrane components. *Proc. Natl. Acad. Sci. USA.* 74:2909–2913.
39. Gross, D., and W. W. Webb. 1983. Time lapse video recording of individual molecular motions of LDL-receptor complex on living human fibroblasts. *Biophys. J.* 41(2, Pt. 2):215*a*. (Abstr.)